Rev. Int. Contam. Ambie. 38 (Sustainable Architecture and Urban Environment) 133-148, 2024
https://doi.org/10.20937/RICA.54459

COASTLINE STABILITY ANALYSIS OF ZHOUSHAN-LIUHENG LNG TERMINAL PROJECT BASED ON REMOTE SENSING

Análisis de la estabilidad de la linea costera del proyecto de la terminal LNG de Zhoushan-Liuheng con base en percepción remota

Ming GONG[1]*, He ZHANG[1] and Yanning LI[2]

[1]Second Institute of Oceanography, MNR, 36 Baoshubei Road, Hangzhou, China, 310012.
[2]National Marine Data and Information Service, 93 Liuwei Road, Tianjin, China, 300171.

*Author for correspondence: juegongk721862@163.com

(Received: June 2021; accepted: October 2021)

Key words: Seabed, sensing images, pipeline.

ABSTRACT

Seabed evolution research around Zhoushan Liuheng LNG receiving station project, which mainly includes collecting, analyzing and sorting data of environmental investigation, was conducted by the second Institute of Oceanography, MMR. Based on the data of remote sensing and field survey for different years, the comprehensive research methods of dynamic geomorphology, sedimentology, stratigraphy and mathematical simulation are used to carry out the geomorphological investigation of the sea area near the Zhoushan Liuheng LNG terminal project. This paper makes a detailed analysis of the beach dynamics, seabed scouring and silting change characteristics of the project sea area, and makes a prediction of the beach channel scouring and silting adjustment trend caused by sea related projects, which provides a scientific basis for optimizing the plane layout of Zhoushan Liuheng LNG receiving station project and insight for other researchers who focus on coastline change and remote sensing.

Palabras clave: Lecho marino, imágenes de percepción, ductos.

RESUMEN

El Segundo Instituto de Oceanografía, MNR, llevó a cabo una investigación sobre la evolución del lecho marino alrededor del proyecto de la estación receptora de GNL Zhoushan Liuheng, que incluye principalmente la recolección, análisis y clasificación de datos de investigación ambiental. Para lo anterior, se utilizaron métodos exhaustivos de geomorfología dinámica, sedimentología, estratigrafía y simulación matemática. Este documento hace un análisis detallado de la dinámica de la playa, el arrastre de los fondos marinos y las características de cambio de los sedimentos de la zona de mar del proyecto. Asimismo, hace una predicción de la tendencia de ajuste del canal de playa causado por proyectos relacionados con el mar, lo que da una base científica para optimizar el diseño del plano del proyecto de la estación receptora de GNL Zhoushan Liuheng y aporta resultados para los investigadores que se estudian los cambios en las costas y la teledetección.

INTRODUCTION

Nowadays the shortage of land resources in the coastal zone has become an urgent problem. At the same time, the rapid expansion of coastal resources development has brought great pressure to the coastal ecological environment and coastal wetlands. For example, overexploitation leads to the disappearance of the natural landscape in the coastal zone, the serious destruction of ecological environment and resources including coastline, tidal flat and wetland, and frequent coastal disasters.

The research on shoreline mainly concentrated in estuaries, harbors, and other areas with large shoreline changes, such as the estuary area of the Nile Delta (White and El Asmar 1999), Gomso Bay (Ryu et al. 2002), beaches of Tamil Nadu and Puducherry in southeast India (Muthusankar et al. 2016), Nestos Delta (Anastasiou and Sylaios 2016), and Jijelian coast of Algeria (Kermani et al. 2016). Rahman (2011) found that the Songdaban coastline showed a trend of erosion-rapid deposition-slow deposition from 1973 to 2010. In the recent 37 years, the erosion area along the outer edge of the estuary delta was 170 km (Ryu et al. 2002). Satellite images were used by Vinayaraj (2011) to study Kali, Sharavathi, Kollur-Chakkara Haladi, and Udyavara along the coast of Karnataka, India. Results showed that erosion and deposition exist at the same time for the four estuaries, and erosion mostly occurs locally and discontinuously.

The coastline dynamic change monitoring is mainly based on extracting the coastline of relevant areas, studying the dynamic characteristics of coastline, erosion and siltation, and analyzing the causes of change. Chowdhury (2013) used multi-temporal topographic maps and Landsat satellite images to measure the coastal erosion and accumulation of Pak Phanang in southern Thailand from 1973 to 2003, in which the land accumulation and erosion were estimated (Chusrinuan et al. 2009). Tran Thi V analyzed the coastline in the south of Vietnam using aerial data (1953), Landsat series data (1979, 1988 and 2000), spot satellite remote sensing data (1992, 1995, 2004, 2008, 2009 and 2011) and digital coastline analysis system (DSAs). The results show that the linear regression rates of erosion in the East China Sea and accumulation in the Gulf of Thailand are 33.24 m/yr and 40.65 m/yr, respectively (Tran Thi et al. 2014). There are also other reports on shoreline erosion and other changes caused by sea level rise (Vongvisessomjai et al. 1996).

Finlayson evaluated and monitored the tropical coastal wetland ecosystem in Australia (Finlayson 2001). Dellepiane et al. (2004) proposed an InSAR Coastline Extraction Method Based on fuzzy connectivity and consistency measurement. Robinson (2004) analyzed the coastline change pattern of a certain area from 1941 to 1991 using aerial photography and topographic maps. Evaluation and quantitative analysis were conducted by Yagoub and Kolan (2006) to study the land use/cover change of Abu Dhabi coastal zone from 1972 to 2000 using Landsat image data of multiple time phases. Supervised classification and expert visual interpretation were used to classify the images, analyze the types and areas with significant changes, and explore the main driving forces.

In recent years, temperature rise and precipitation change have become the main meteorological factors affecting the distribution and pattern of coastal wetlands. Scholars around the world have done a lot of research on the impact of climate change and human activities on the coastal zone. IPCC (2007) report reveals that under global climate change, the coastal wetland is the most sensitive area to respond to climate change, so it can be used as an important indicator of climate change research. Snoussi et al. (2008) selected sea-level rise rate, daily average flooding time and intertidal habitat elevation to evaluate the vulnerability of the eastern Mediterranean coastal ecosystem under the influence of sea-level rise. Abuodha and Woodroffe (2010) evaluated the vulnerability of the coastal zone in southeastern Australia, aiming to study the impact of sea-level rise on the coastal zone qualitatively and quantitatively, so as to formulate measures to slow down sea level rise. Hadipour et al. (2012) established a spatial model for the location of seawall by the geographic information system (GIS), remote sensing (Muthusankar et al.) and global positioning system (GPS), which improved the land use value. Using remote sensing and chart data, Choi (2014) reviewed the history of coastal tidal flat reclamation in South Korea from 1950s to 2000s, and discussed the relationship between large-scale reclamation activities and socio-economic policies, as well as their impact on tidal flat morphology. Natesan et al. (2015) monitored and analyzed the coastline changes of Tamilnadu, India, using remote sensing and DSAs module developed by the United States Geological Survey (USGS). Based on the supervised classification method and GIS technology, Esmail et al. (2016) studied the land use and cover change in the Nile coastal zone, and the impact of land use change on the environment.

Most of the existing studies generally focus on obtaining intuitive shoreline change results by remote sensing, while research combined with local hydrological and sediment environment is still in lack. Combined with the local hydrological and underwater topographic observation results for many years, this research demonstrates the impact of local human reclamation activities on coastline change.

MATERIAL AND METHODS

Methods

The relevant reports and data on the preliminary environmental investigation and research of the Zheneng Zhoushan Liuheng LNG receiving station project was collected; an on-site survey and survey to supplement the geomorphological investigation of the sea area near the project was conducted.

According to the topographic survey, hydrology, and sediment of the project sea area in different years combined with the previous research results and the comprehensive research methods of dynamic geomorphology, sedimentology, stratigraphy, and mathematical simulation, this research carried out a detailed analysis of the beach dynamics, suspended sediment distribution and migration trend, and seabed scouring and silting change characteristics of the Liuheng LNG receiving terminal project sea area. It predicted the scouring and silting trend caused by sea-related projects. This research provided a scientific basis for optimizing the plane layout of the Zhoushan Liuheng LNG terminal project.

Landform condition

Zhejiang Zheneng Liuheng LNG Co., Ltd. LNG terminal is located in Liuheng Island of Zhoushan. The terminal is located in the area surrounded by Qingshan - Liqingshan - Xiaoyangzhishan - Paotaigang - Baimajiao reclamation area inside Xiaoguoju phase II reclamation area on the south side of Liuheng Island, as is shown in **figure 1**.

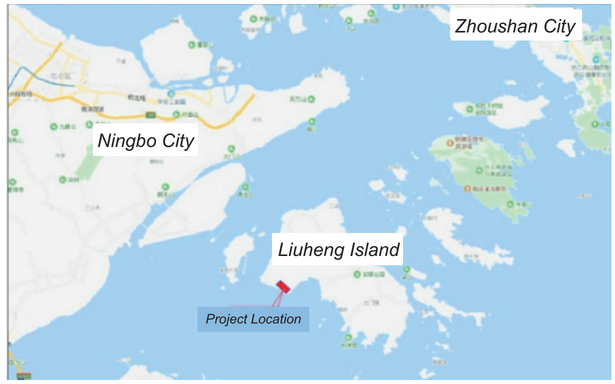

Fig. 1. Location map of Zheeneng Zhoushan LNG terminal.

The proposed Liuheng LNG terminal project mainly includes three parts: gas pipeline project, wharf project, and terminal project (land part). The first is the gas transmission pipeline which mainly includes a 37 km long sea-crossing gas transmission pipeline connecting Liuheng Island and Chunxiao station of Zhejiang natural gas pipeline network (including about 19 km of the offshore pipeline), as well as supporting valve chambers and stations on land. The second is the wharf project, including a 150 000 DWT (Vongvisessomjai et al.1996) LNG Wharf and a 2000 DWT working ship wharf (with construction material wharf) and corresponding supporting projects. The third is the terminal project (land area). The terminal is located in the area surrounded by Qingshan-Liqingshan-Xiaoyangzhishan-Paotaigang -Baimajiao reclamation area inside Xiaoguoju phase II reclamation area on the south side of Liuheng Island. The submarine gas pipeline of LNG terminal project goes to the sea from the northwest end of Guojudi of Liuheng Xiaoguoju reclamation phase II project, approximately vertically crosses the south channel of Liuheng (near point D) to AC1-1 to the southwest, and then turns westward to cross the deep channel slope (near section AC1-2) to the south of Shuangyumen waterway, extending to the north of the submarine pipeline monitoring route of Chunxiao gas field group. It lands at about 25 m to the northeast of the landing point of a submarine pipeline of Chunxiao gas field group. The total length of the route is 19.376 km. The specific location is shown in **figure 2**.

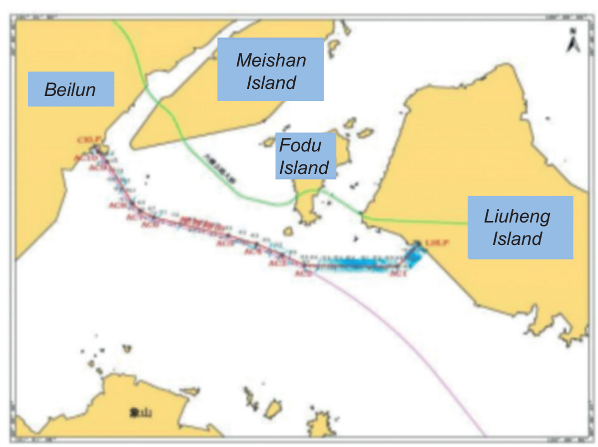

Fig. 2. Location of terminal station and pipelines.

The route is located in the sea area between the southwest of Liuheng Island and Chunxiao of Beilun. From east to west, it successively passes through Niubishan waterway and Xiangshan gangmen shoal area. The seafloor is basically flat, and most of the water depth is within 10 m. However, in the south entrance of Shuangyumen waterway on the west side of Liuheng Island, the route passes through the tail part of the deep channel scoured by a tidal current of Shuangyumen waterway, with relatively large water depth and complex terrain field. The variation of water depth and topography in the route area is shown in **figure 3**.

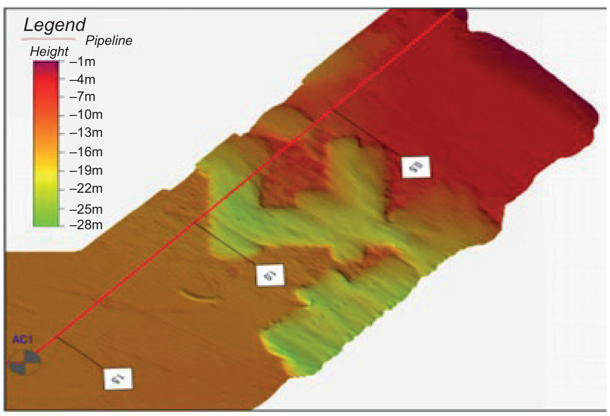

Fig. 3. Seabed topography.

From KP0.5-KP1.2, the water depth varies greatly due to manual sand blowing, with a maximum water depth of 25.2 m. The local seabed topography is complex (**Fig. 3**). Therefore, engineering measures should be taken for submarine pipeline laying. The southeast end of the scour trough in the southwest front of Guojushan reaches the route area, and the maximum water depth in the area is about 16 m. Due to the continuous shrinkage of the scour trough in recent years, the safety of the submarine pipeline will not be affected.

In Oct.~Nov., 2019, the Second Institute of Oceanography of the Ministry of Natural Resources arranged 9 fixed-point hydrometric stations and 1 temporary tide gauge station in the sea area near the survey route, in which data of 3 long-term tide gauge stations (Xize station, damutu station and Zhinan station) nearby was collected. The station layout is shown in **Fig. 4**.

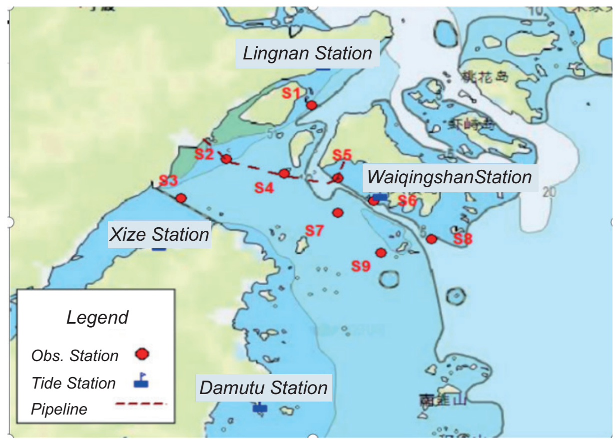

Fig. 4. Location of observation stations.

Marine hydrodynamic conditions

Tide and wave

The ratio of diurnal amplitude and main semi-diurnal component is less than 0.5, indicating that the tide type is a regular semidiurnal tide. The tidal level and height are shown in **table I**. During the autumn observation, the maximum measured tidal

TABLE I. TIDAL CHARACTERISTICS (UNIT: m).

		Xize	Chinan	Damutu	Waiqingshan
Tidal level	Maximum tide level	2.97	2.33	2.71	2.71
	Minimum tide level	–2.38	–2.24	–2.29	–2.20
	Mean high tide level	1.91	1.46	1.71	1.69
	Mean low tide level	–1.01	–0.89	–1.12	–1.05
Tidal height	Maximum tide height	0.30	0.29	0.28	0.28
	Maximum tide height	3.94	4.04	4.65	4.58
	Mean tide height	0.54	0.53	0.75	0.67
Tide time	Mean time of tide	2.53	2.36	2.85	2.76
	Mean timeof edd	6h 41m	5h 42m	5h 59m	6h 08m
Observation period		2019.10.23~11.23			

current velocity of 9 stations (S1-S9) in the project sea area is 1.45 m/s, which appears at the S1 station. The maximum vertical average current velocity is 1.34 m/s at the S9 station.

According to the tidal current vector diagram (**Fig.5**), the tidal current direction for the nine stations is relatively regular, showing obvious reciprocating flow characteristics except for the S4 station. The rising tide flow direction of the S4 ~ S9 station is basically northwest while the falling tide is southeast. For the S2 station, the rising tide direction is basically southwest. The rising tide flow direction of the S1 station is northeast, while that of falling is southwest.

Zhoushan sea area, close to the East China Sea, is a big wave area in China's coastal area. Affected by the monsoon, the waves are mainly northward in winter when the wave height is larger. In summer, the waves are mostly southward, and the wave height is smaller than that in winter. The typhoon wave is the largest wave in a year. In Xiashimen sea area, the normal wave direction is ESE and the strong wave direction is N with an annual mean wave height 0.9 m, annual average period 3.9 s, maximum wave height 4.6 m, and maximum wave period 8.5 s.

According to the observation data of long-term wave stations (29º3'47.0" N, 122º21'52.4" E) in the nearby sea area from January to December 2011, the annual average value of effective wave height (H_S) is 0.71 m, which is the highest in September and the lowest in January and March. Effective wave height refers to the actual wave height of the first n/3 waves.

The maximum value of H_1/H_{10} is 10.75 m in August, and the second maximum value is 8.76 m in June, corresponding to the transit period of the tropical storms Mire and Meihua, respectively. The annual average period T_a is 6.9 s, and the longest period is 12.3 s in September. The waves with an average period of more than 5 s account for 98%, which means that the engineering sea area is dominated by long-period waves.

The wave with the direction of ENE-E-ESE-SE accounts for 88.9% of the whole year. In spring, the waves in E direction, accounting for 33.7%, appears most frequently. In summer, the waves in SE direction occupies the controlling position. In autumn, the waves in ESE direction and E direction are the most frequent. In winter, the waves in ENE direction and E direction account most.

Sediment

The variation of suspended sediment concentration is an important manifestation of sediment transport, deposition and re-suspension under hydrodynamic action. Nine fixed-point tidal current stations (No. S1-S9) were set up in this hydrological observation. From Nov. 5 to Nov. 13, 2019, hydrological and sediment observations were carried out for large, medium and small tides, each of which was observed for 27 hours continuously. Suspended sediment-water samples were sampled in layers at the surface, 0.6 m water depth and bottom. Water

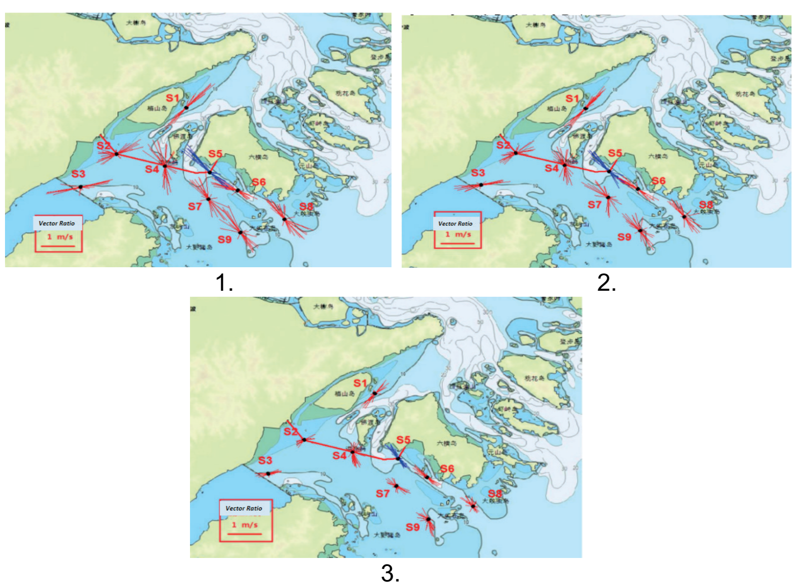

Fig. 5. Vertical mean flow vector (1: high tide 2: median tide 3: lower tide).

samples were collected with a water collector per layer each hour

According to the measured data, the average sediment concentration in this area is 0.227 kg/m^3, and the vertical average sediment concentration is 0.052-0.749 kg/m^3. The measured sediment concentration in the engineering sea area varies from 0.994 kg/m^3 to 0.012 kg/m^3, respectively.

The maximum sediment concentration of a single point in the flood period table and bottom layer is 0.535 kg/m^3 and 0.994 kg/m^3 respectively, which occurs in the high tidal period of the S2 station, and the minimum values are 0.014 kg/m^3 and 0.062 kg/m^3 respectively, which occurs in the low tidal period of S5 station and S6 station.

The maximum sediment concentration for surface and bottom during the rising tide period is 0.488 kg/m^3 and 0.980 kg/m^3, which occurs at high tides of S7 station and S3 station respectively. The minimum values are 0.012 kg/m^3 and 0.046 kg/m^3, which appears at S6 and S3 station during low tides.

Sediment discharge is a combination of flow rate and sediment concentration. The sediment discharge per width is proportional to the flow velocity, sediment concentration, water depth and time, which reflects the weight of the average sediment concentration through the 1 m width vertical section. From the calculation results, the sediment discharge per width for the high tide is the highest while the low tide is the lowest (see **Table II**).

TABLE II. SEDIMENT DISCHARGE PER UNIT WIDTH AND DIRECTION OF EACH STATION.

Station	Tide	Rising		Falling		Net sediment transport	
		Sediment Transport (t/m/d)	Direction (º)	Sediment Transport (t/m/d)	Direction (º)	Sediment Transport (t/m/d)	Direction (º)
S1	High	125.6	41	66.7	221	58.9	40
	Medium	95.9	39	71.8	222	24.5	30
	Lower	19.4	42	26.0	220	6.7	214
S2	High	42.4	264	34.6	63	16.1	315
	Medium	25.0	244	18.8	57	6.8	264
	Lower	6.6	246	4.3	88	3.1	214
S3	High	159.2	255	90.0	79	69.6	251
	Medium	80.9	258	47.1	77	33.8	261
	Lower	6.9	261	6.7	82	0.2	243
S4	High	154.9	352	76.7	170	78.2	353
	Medium	55.9	351	35.6	168	20.6	358
	Lower	19.5	14	32.1	164	17.9	132
S5	High	215.4	320	87.4	127	131.5	328
	Medium	78.4	321	34.4	131	45.0	329
	Lower	29.7	330	15.9	134	15.0	346
S6	High	161.6	290	78.8	122	86.4	278
	Medium	117.6	307	71.3	132	46.9	300
	Lower	45.5	313	35.7	127	10.6	333
S7	High	105.1	325.9	86.5	137.7	23.0	358.1
	Medium	51.0	317.7	24.9	159.3	29.4	299.5
	Lower	13.4	310.3	15.3	129.1	1.9	120.6
S8	High	120.2	331.3	115.4	130.5	42.7	44.6
	Medium	64.4	333.6	39.0	136.5	29.4	356.6
	Lower	27.3	328.7	11.4	146.2	15.9	330.5
S9	High	113.4	324.0	63.5	140.3	50.2	328.8
	Medium	56.9	326.1	47.2	143.8	9.9	337.3
	Lower	27.1	300.0	30.5	166.7	23.1	225.6

RESULTS AND DISCUSSION

Recent coastline evolution

The reclamation works near the landing section of Liuheng include Xiaoguoju phase I works and phase II (**Fig. 6a**). Xiaoguoju phase II reclamation Project is located in the southwest of Lighting Island. The main part of Guoju dike was built in 2011 and completed in 2015. However, there are ports left in the middle which was closed completely in 2018. It became a new coastline after the construction. Remote sensing images from different periods were taken, from which the changes of the surrounding works and coastline in different periods are shown (**Fig. 7a**).

Reclamation works near Chunxiao landing section mainly include Qixingtu reclamation on the south side of Meishan Island (completed in 2011), Yangsong Tu reclamation (completed in 2019) and the South Embankment of Meishan Waterway Project (completed in 2017) (**Fig. 6b**). Remote sensing images from different periods can clearly show the changes of coating works and coastlines in different periods (**Fig. 7b**).

Southwest sea area of Liuheng Island

By comparing the contour distributions of 0 m, 2 m, 5 m, 10 m and 20 m in 1963, 2005 and 2012, the flat changes of tidal flats and deep troughs along the sea area are analyzed.

It can be seen from **figure 8a** that after the implementation of Guojushan phase I, two bays, one large and one small, are formed on both sides of the reclamation area, in which the LNG receiving station project is located on the west side of Guojushan.

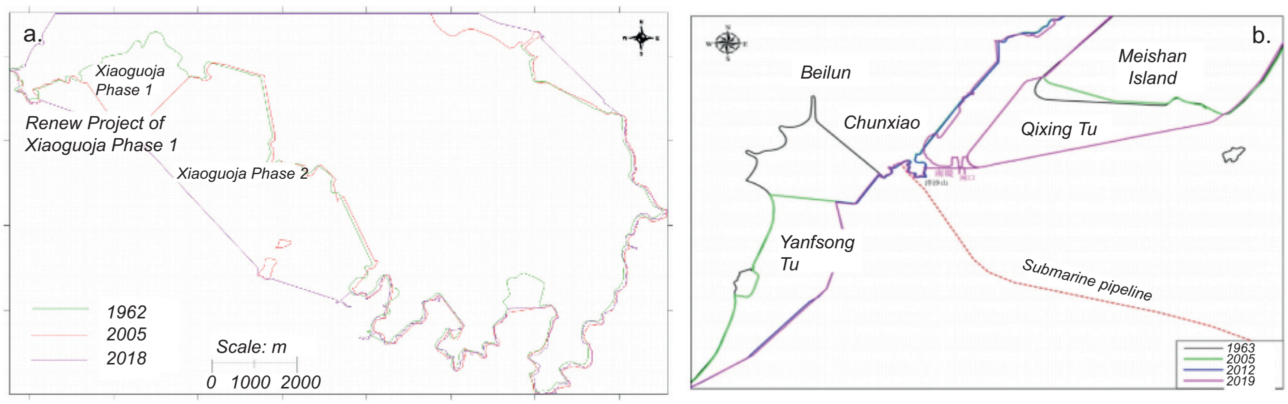

Fig. 6. Change of coastline (a: South of Liuheng Island; b: Chunxio landing section).

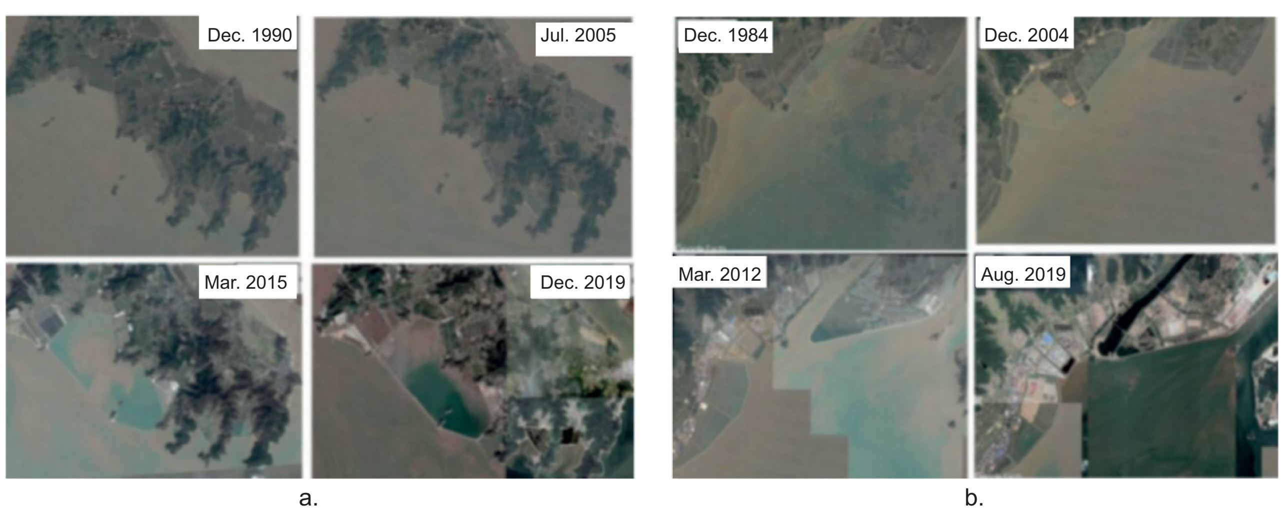

Fig. 7. Remote sensing images (a: South of Liuheng Island; b: Chunxio landing section).

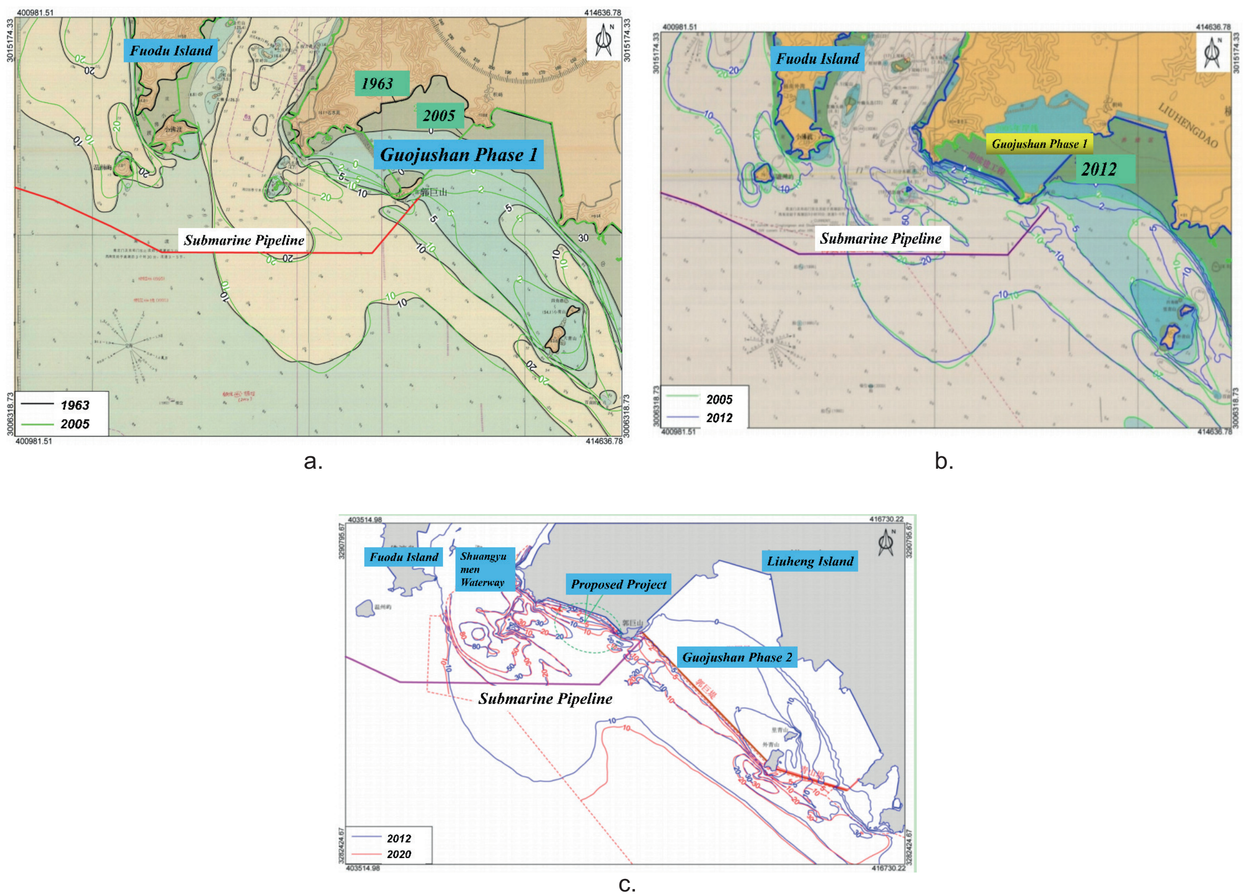

Fig. 8. Coastline change in the southwest of Liuheng Island (a: 1963-2005; b: 2005-2012; c: 2012-2020).

Significant silting occurred in the two bays with the 0 m contour moving outward to the sea. The deep trough area between Xiaoqingshan and Liuheng Island is mainly silted and the 5 and 10 m contours shrink toward the middle of the deep trough. Due to obvious deflecting action and enhanced hydrodynamic force, erosion occurs on the south side of Guojushan. The 20 m contour at the southern end of the Shuangyumen waterway tends to move outwards. The 10 m contour in the outer sea area far from the reclamation area has little change.

Figure 8b shows the contour lines of 2005 and 2012. The phase I renewal project of Guojushan was implemented in 2012, straightening the coastline of the west side of Guojushan. The proposed LNG terminal and drainage works are located in the offshore area of the embankment. Due to the construction of the sea embankment, the 0 m contour line in this area is extrapolated as a whole, while the position of the 2 m, 5 m, 10 m and 20 m contour lines on the outside changes little as a whole. Erosion is still dominant on the south side of Guojushan Mountain, and the 10 m contour moves eastward. In addition, there are artificial sand mining activities in the sea area. Deep pits were formed after sand mining and the 10 m contour moved to the shore locally. During this period, the bay on the east side of Guojushan phase I reclamation was still mainly silted, and 0 m, 2 m and 5 m contours partly moved towards the sea. The 5 m and 10 m contours of the deep trough on the northeast side of Liqingshan Mountain shrink toward the middle of the deep trough. The contour lines of 20 m and 30 m at the southern end of Shuangyumen waterway show little change, and there is a tendency to move towards deep trough locally. The seabed in the outer sea area far from the reclamation area is relatively stable, and the position of the 10 m contour line does not change much.

Figure 8c shows the contour lines in 2012 and 2020. The Guojushan Project phase II has been completed in 2020. The construction of Guoju dike and Qingshan dike has resulted in great changes in the entire surrounding area terrain. After reclamation, the deep trough on the east side of Castle Peak disappeared, and silting of different scales occurred on the outside of the embankment. The 5 m contour on the outside of Castle Peak embankment basically runs parallel to the embankment. The 5 m contour line of Guojudi moveed outwards, especially on the southeast side of Guojushan, where the maximum movement is 380 m. The dock and drainage works of the proposed LNG receiving station project are located in the outer sea area of the embankment on the west side of Guoju Mountain. The sea area's 5- and 10 m contours have also been extrapolated obviously, and the outer deep trough area's 20 m and 30 m contours have shrunk to the middle and deep parts. The 10 m and 20 m contours in the south side of Guojushan sand mining area were irregularly distributed in the two periods. The shape of 20 m and 30 m contours at the southern end of Shuangyumen Waterway has changed little, of which the 20 m contour has a tendency to move outwards locally. The outer sea area far from the reclamation area is scoured and the 10 m contour moves southward.

Submarine pipeline routing area

Based on the topography data in 1963, 2005, and 2012, the horizontal changes of a tidal flat and deep trough along the coast were analyzed. The sea area was mainly silted from 1963 to 2005 (**Fig. 8**). A reclamation area formed in the northern part of Yangsongtu on the west side of the Chunxiao landing site where the coastline has moved outward. The bathymetric contour of 0 m, 2 m and 5 m in front of the coastline has all moved to the open sea, of which the 5 m contour has a maximum distance of 1.7 km. The tongue-like tidal flat in the south of Meishan Island tends to expand outward, and the 10 m contour in the southeast deep trough area of Meishan Island moved to the deep trough. Sedimentation has also occurred in the sea area near Wenzhou Island, for the contour has moved to the northeast.

During 2005-2012 (**Fig. 9**), Yangsongtu and Qixingtu to the south of Meishan Island were reclaimed on a large scale with coastline moved to the open sea by a large margin. The 0 m and 2 m contour of the shoreline move to the open sea, and the 5m contours move eastward for a large distance up to 2.1 km. The 10 m contours in the southeastern deep trough of Meishan Island moved further to the deep trough. The deep trough on the west side of Wenzhou Island is locally scoured.

Submarine pipeline seabed

Based on the topography data in 2012 and 2020, the scouring and silting calculation of the sea bed in the route area was carried out. The results show that in the past eight years, the areas with great change amplitude mainly appear in the coastal route area, especially in the coastal section of Liuheng Island. Influenced by the reclamation project of Xiaoguoju phase I and phase II, large-scale siltation occurred in the sea area outside the seawall where the pipeline landing point is located. The siltation amplitude in the deep trough area on the south side of Guoju Mountain is the largest, with the maximum siltation of 13.0 m and siltation rate of 1.6 m/a. In addition, the pipeline route in the nearshore section passes through an area where the water depth has increased significantly. According to the investigation, there have been artificial sand mining activities in the sea area outside the reclamation area in recent years, causing many deep pits on the seabed. According to the topographic comparison between 2012 and 2020 (**Fig. 10**), a large-scale sand mining area has

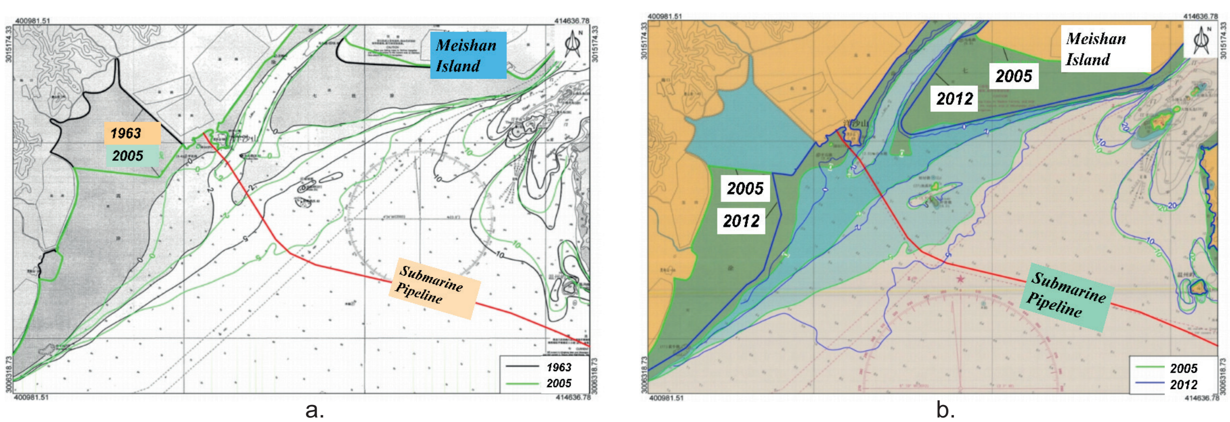

Fig. 9. Change of annual contour in subsea pipeline routing area (a: 1963-2005; b:2005-2012).

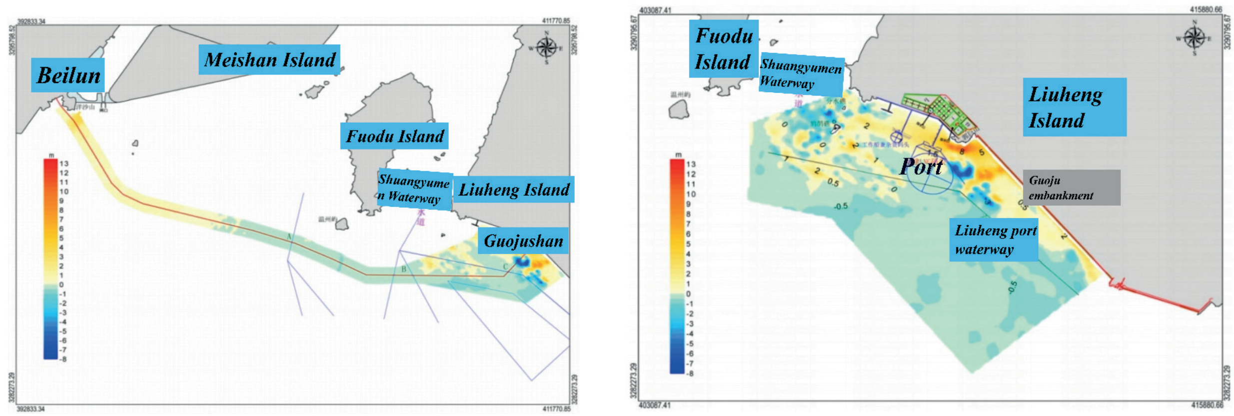

Fig. 10. Distribution of seabed scouring and silting around subsea pipeline and the drainage works (2012-2020).

existed in the southeast of the route area in 2012. The topographic map of 2020 shows that the sand mining area experienced rapid deposition to achieve a new balance. After that, the sand mining area extended to the northwest. There are many deep holes after all the sand mining on the seabed.

It can be seen that deposition has occurred in the eastern part of the local sand mining area. Local siltation occurred in the route area at the south end of Shuangyumen waterway with a siltation range of 0~2.0 m. The deep-water area on the south side of the waterway where the pipeline route passes experienced a slight scouring whose range is less than 1.0 m. The route area on the south side of Wenzhou Island is slightly scoured with scour amplitude less than 0.5 m. The terrain in the middle route area of the pipeline is smooth, showing a relatively balanced state of erosion and deposition. The route area in the nearshore section of Yangshan Mountain is mainly silted up, which is mainly related to constructing a sea gate between Yangshan Mountain and Meishan Island, which blocks most of the water body. Moreover, the large-scale reclamation of Yangsongtu on the south side of Beilun Mountain led to the obvious siltation of the nearshore area. For the south side of Yangshan Mountain, the deposition range is relatively large, with a maximum of 4.0m, and the deposition rate is 0.5m/a.

Sea area near docks and drainage works

Souring and silting of the seabed near the wharf and drainage works is calculated using the water depth and topographic data in 2012 and 2020. As is shown in **figure 10**, affected by the continuous reclamation project of Xiaoguoju phase I (completed in 2013) and II (completed in 2018), large-scale silting occurred in the outer sea areas of the renewal embankment phase I and Guoju embankment. The southern deep trough of Guojushan has the most considerable silting extent, with a maximum of 13.0 m and silting rate of 1.6 m/a. The intake and drainage pipeline project is close to the sea embankment. Affected by reclamation, this area is mainly influenced by silting, in which the silting range is 3.0 m and that at the outlet is 1.0 m, as shown in **figure 11**.

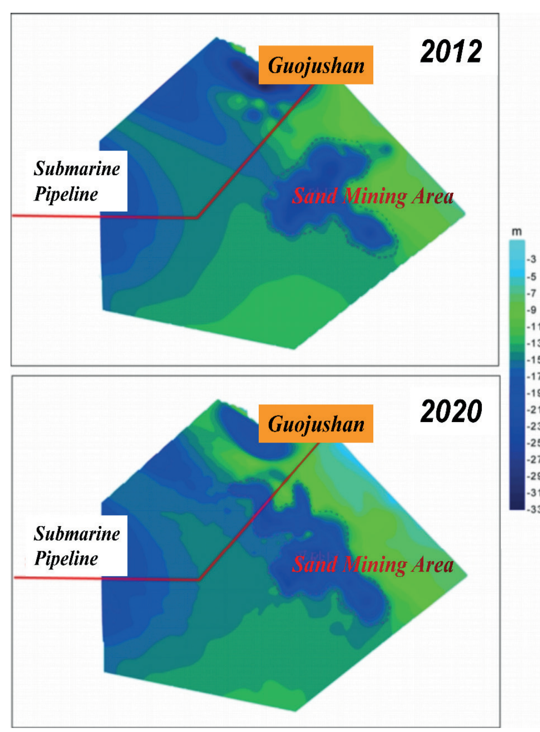

Fig. 11. Underwater topographic map near Liuheng Island landing section (2012 and 2020).

Typical section

Taking the subsea gas pipeline of this project as the representative section, the scouring and silting changes of the section configuration of the subsea gas pipeline are analyzed. The pipeline location distribution is shown in **figure 12**. In addition, three typical profiles are arranged in the measuring area of the proposed pier and the sea area where the intake and drainage works are located (**Fig. 13**). The underwater topographic data of 2012, 2019 and 2020 are used to analyze the annual scouring and silting changes of the seabed.

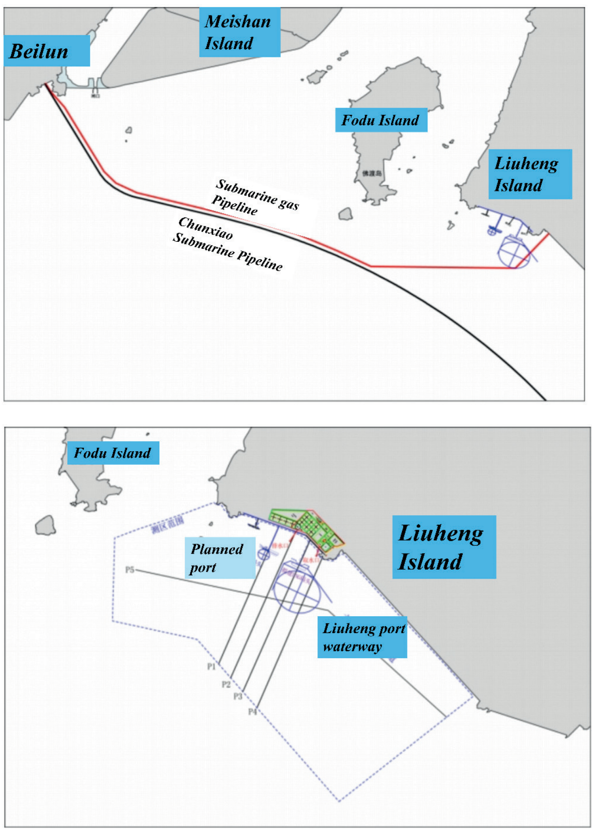

Fig. 12. Planned port and submarine gas pipeline.

Submarine gas pipeline route profile

Taking the subsea gas pipeline route as the representative section, the topographic change of route section from 2012 to 2020 is drawn (**Fig. 14**). It can be concluded from **table III** that siltation occurs in the front of the Liuheng landing point with a range of 0-6.0 m and an average annual range of 0-0.75 m. Due to the influence of artificial sand mining activities, the water depth suddenly increases for some areas, which can reach 8 m. The deep channel and the slope areas at the south end of the Shuangyumen waterway are slightly scoured, and their scour amplitude is less than 0.5m. The terrain of the flat route area to the west is unchanged, with its seabed relatively stable. The underwater shoal area of Xiangshan Harbor gate is slightly silted. The siltation amplitude of the sea area outside the Chunxiao landing site is larger, where a small deep pool becomes flat. Generally speaking, the terrain changes are small except for the Liuheng Nearshore Area, which is influenced by sand mining.

Typical sections near the proposed wharf and water drainage works

P1, P2, P3 sections cross-dock the platform vertically. By comparing the underwater topographic data in 2012, 2019 and 2020, it is seen that there are obvious topographic changes in these periods (**Fig. 15**). Affected by reclamation, obvious silting occurs in the near-shore slope and deep trough area. The silting range of the underwater slope area is 0-2.0 m in 2012-2020 and 2012-2019, indicating little topography change during 2019-2020. The scouring and silting in the outer sea area of the adjacent reclamation works gradually reached a new equilibrium state. The terrain in the outer deep-water area fluctuates and scours locally. From 2012 to 2020, the outer sea area of this section is mainly dominated by scouring with a range of 0-1.0 m. Similar to section P1, there is an obvious geomorphic change in three periods for the P2 section. The silting range in the near-shore slope and deep trough area is 0-3.0 m during 2012~2020. The offshore deep trough area silting range is 0-2.0 m during 2012-2019 while the slope and deep trough area topography change little during 2019-2020. The terrain of outer deep-water area is undulating with a scouring range of 0-2.0 m from 2012 to 2020. During 2012-2020, the outer sea area of this section is mainly scoured with a scouring range of 0-1.2 m.

Huge geomorphic change for P3 in the three periods was observed. The silting range is 0-4.0 m for the near-shore slope area in the period of 2012-2020. Water depth in the proposed platform for grocery terminals was 17.0 m in 2012 and 14.0 m in 2020. The terrain of the outer sea area is relatively flat, which is mainly scoured during 2012-2020.

P4 section is a vertical route crossing the deep trough area on the south side of Guojushan. Obvious geomorphic changes occurred in the three periods. The maximum silting range can reach 9.0 m in 2012-2020. The terrain of the outer sea area is relatively flat.

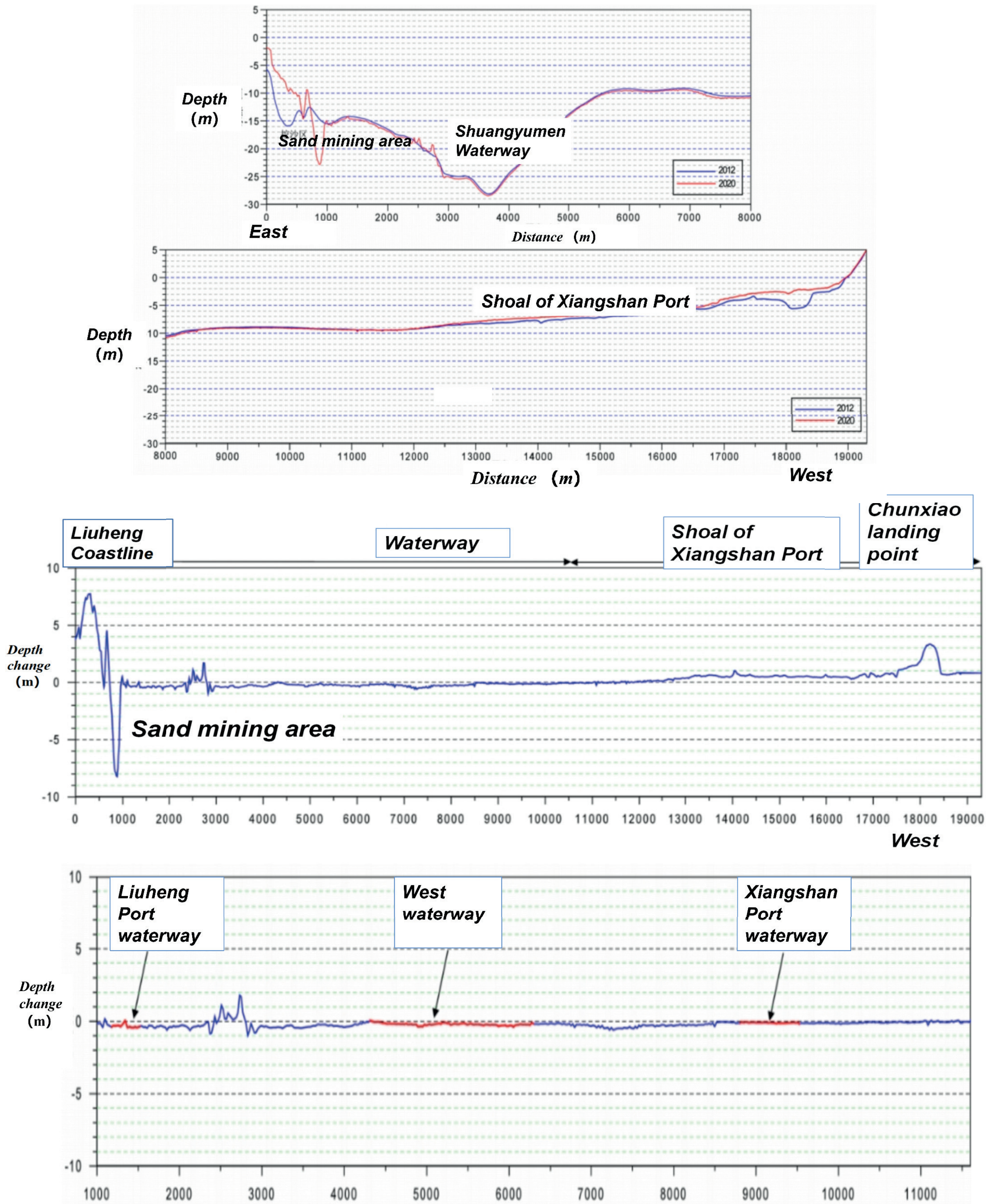

Fig. 13. Topographic change of submarine gas pipeline route section, submarine gas pipeline, channel anchorage scouring section in route area from 2012 to 2020.

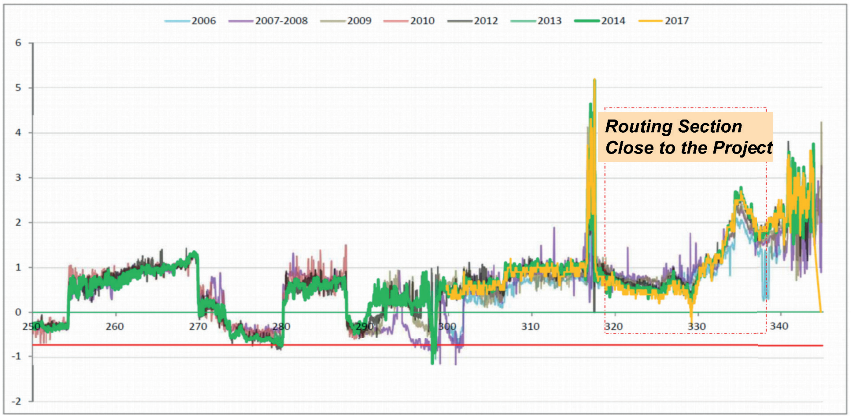

Fig. 14. Comparison of the buried depth of submarine pipeline KP250-KP345 in Chunxiao gas field group.

TABLE III. SCOURING AND SILTING CHANGES OF SUBMARINE GAS PIPELINE ROUTE AREA FROM 2012 TO 2020.

Route mileage to Liuheng landing point (km)	Annual scouring and + silting range (cm)	Position	The annual scour amplitude corresponding to the larger scour position
KP0~0.7	57.1	Liuheng nearshore section	——
KP0.7~1.1	–42.5	Sand digging area	KP0.88 (103 cm) caused by sand mining
KP1.1~2.4	–4.6	Approach channel area on the south side of Liuheng	KP1.4 (5.8 cm)
KP2.4~2.8	6.9	North slope of Shuangyumen	——
KP2.8~11.6	–2.7	Deep water channel area	KP2.9 (12.2 cm)
KP11.6~17.0	5.4	Xiangshan port shoal	——
KP17.0~19.0	16.7	Chunxiao landing point	——

Note + presents silting - presents scouring.

Section P5 runs along the Liuheng south approach channel. According to the underwater topographic data in 2012, 2019 and 2020, it can be inferred that the channel changes greatly from west to east, with larger water depth in the west and smaller in the east (**Fig. 15**). Since it is relatively far from the coastline, P5 is less affected by reclamation works. The topography changed little over the three periods, while the topography of the sand mining area changed.

Generally speaking, the evolution of seabed scouring and silting is mainly affected by the reclamation of marginal beaches and artificial sand mining. Affected by Guo Jushan reclamation Project phase I and II, the sea area of Liuheng station is mainly silted with a silting range of 0-6.0m. On the outside of the Guojushan reclamation area, there are several areas where water depth increases significantly, mainly due to artificial sand mining. The deep-water area on the south side of Shuangyumen Waterway where the pipeline routing passes is scoured slightly with an less than 1.0 m. According to the annual routing survey data of submarine pipelines in adjacent Chunxiao gas field, it is suggested that pipeline tracking detection be strengthened because local bareness occurs in this area. The terrain changes little in the underwater area of Xiangshan Port Gate and the seabed is relatively stable. Affected by the nearby reclamation project, the routing area of the Chunxiao landing section is mainly silting. It can be seen that human activities mainly control the evolution of the seabed in the

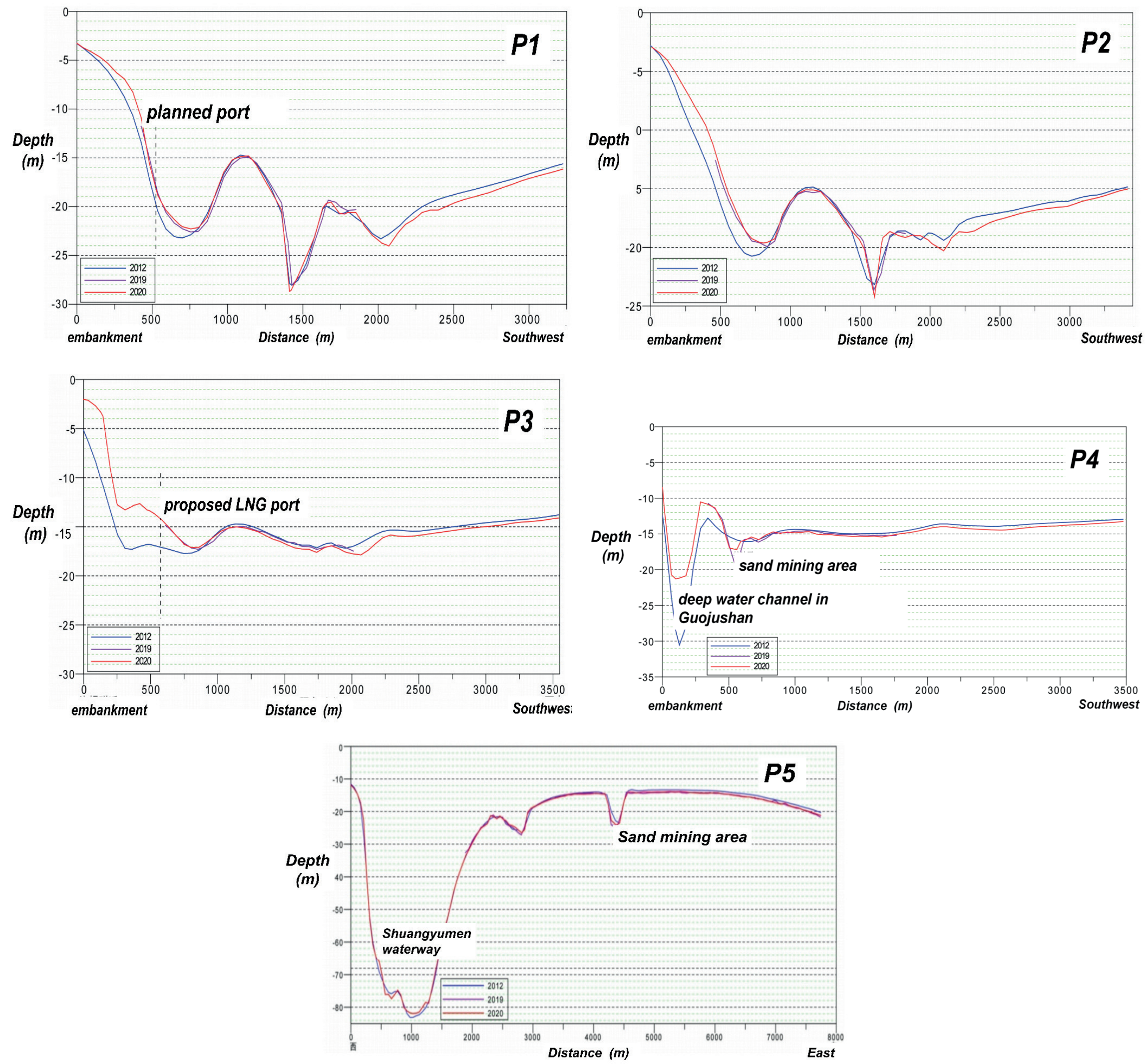

Fig. 15. Underwater terrain for P1 to P5 from 2012 to 2020.

routed sea areas in the recent ten years. The implementation of Xiaoguoju phase I and phase II large-scale silt-promoting and land-making works on the south side of Liuheng Island significantly influences the hydrodynamic and sediment environment in the adjacent areas. Data for 2012 before reclamation and 2020 data after reclamation was used to calculate scouring and silting. The results show that there is a large amount of silting near the dike. For the outer deep water channel area which is affected by the southward pushing pressure of the dike, the flow is concentrated, enhancing hydrodynamic force, leading to scouring. It can be drawn from the comparison of data from 2019 and 2020 of typical profiles that the topography of the outer deep-water area has not changed much and scouring has occurred in some areas, indicating that the scouring and silting of the regional seabed has gradually reached a new equilibrium state.

CONCLUSIONS

Based on the data of water depth and topography in 2012 and 2020, the scouring and silting calculation of the sea bed has been carried out. In the recent eigth years, in addition to many deep pits in the sea bed outside the reclamation area after sand mining, large-scale siltation has occurred in the sea area outside the first phase of the construction of the dike and

Guoju dike. The proposed terminal area is located in the sea area outside the reclamation dike of phase I. The platform berth and rear approach bridge of the proposed LNG terminal are close to the deep trough in the south of Guojushan, and the siltation range is 0 ~ 5.0 m. The working ship and general cargo wharf are located on the west side of the proposed wharf. The siltation range of the wharf platform berth and the rear approach bridge is 0 ~ 3.0 m, and the siltation rate is 0.38 m/a. The lateral gyration water area of the proposed LNG terminal is mainly silted with a range of 0 ~ 2.0 m, while the lateral gyration water area of the proposed LNG terminal is mainly scoured with a range of 0 ~ 0.5 m. Under the influence of the seawall pushing southward, the past flow is concentrated in the channel area, and the hydrodynamic force is enhanced. The channel area at the south side of Liuheng is mainly scoured, and the scour amplitude is small, about 0 ~ 0.5 m. The water drainage pipeline project is close to the seawall. During this period, it is mainly affected by reclamation, and the siltation range is 3.0 m at the water intake and 1.0 m at the outlet.

Generally speaking, the evolution of seabed erosion and deposition in the project area is mainly affected by beach reclamation and artificial sand mining. Influenced by Guojushan phase I and phase II reclamation project, the sea area outside Liuheng terminal project is mainly silted, with a siltation range of 0-6.0 m. There are several water depth-increasing areas outside Guojushan reclamation area, which are mainly caused by artificial sand mining. The deep-water area on the south side of the channel where the pipeline route passes is slightly scoured, and the scour amplitude is less than 1.0 m. According to the route survey data of the adjacent submarine pipeline in Chunxiao gas field over the years, it is suggested to strengthen the pipeline tracking and detection. The topography of the underwater gentle zone of Xiangshan port gate changes little, and the seabed is relatively stable. Affected by the reclamation project nearby, the route area of the Chunxiao landing section is mainly silted up. It can be seen that the seabed evolution of the route sea area in recent ten years is mainly controlled by human activities, especially the artificial sand mining activities, which cause great topographic relief in the route area. As long as the sand mining activities are stopped in the later stage, the sand pits will continue to deposit. Therefore, it is necessary to prohibit sand mining activities in the sea area before the pipeline construction, and take certain engineering measures to ensure the safety of the pipeline crossing the sand excavation area.

DISCLOSURES

The authors have no relevant financial interests in the manuscript and no other potential conflicts of interest.

ACKNOWLEDGMENTS

This research was funded by Basic Scientific Research Project of Second Institute of Oceanography, MNR. (Funding Number: JG1525)

CODE, DATA, AND MATERIALS AVAILABILITY

Some or all data, models, or code that support the findings of this study are available from the corresponding author upon reasonable request.

REFERENCES

Abuodha P.A.O. and Woodroffe C.D. (2010). Assessing vulnerability to sea-level rise using a coastal sensitivity index: a case study from southeast Australia. Journal of Coastal Conservation 143, 189-205. https://doi.org/10.1007/s11852-010-0097-0.

Anastasiou S. and Sylaios G. (2016). Assessment of shoreline changes and evaluation of coastal protection methods to mitigate erosion. Coastal Engineering Journal 58 (2), 1650006-1650001-1650006-1650024. https://doi.org/10.1142/s0578563416500066.

Finlayson C. M. and Eliot I (2001). Ecological assessment and monitoring of coastal wetlands in Australia's wet-dry tropics: A paradigm for elsewhere? Coastal Management 29 (2), 105-115. https://doi.org/10.1080/089207501750069605.

Choi Y.R. (2014). Modernization, development and underdevelopment: Reclamation of Korean tidal flats, 1950s–2000s. Ocean & Coastal Management 102, 426-436. https://doi.org/10.1016/j.ocecoaman.2014.09.023.

Chowdhury S. R. and Tripathi N. K. (2013). Coastal erosion and accretion in pak phanang, thailand by gis analysis of maps and satellite imagery. Songklanakarin Journal of Science & Technology, 35(6), 739-748.

Chusrinuan N., Tanavud C. and Yongchalemmchai C. (2009). Impacts of shoreline erosion on coastal ecosystems in Songkhla Province. Songklanakarin Journal of Science and Technology 31(2): 34-36.

Dellepiane S., De Laurentiis R. and Giordano F. (2004). Coastline extraction from SAR images and a method for the evaluation of the coastline precision. Pattern Recognition Letters 25 (13), 1461-1470. https://doi.org/10.1016/j.patrec.2004.05.022.

Esmail M., Masria A.L.I. and Negm, A. (2016). Monitoring land use/land cover changes around Damietta Promontory, Egypt, using RS/GIS. Procedia Engineering 154, 936-942. https://doi.org/10.1016/j.proeng.2016.07.515.

Hadipour M., Pourebrahim S. and Mokhtar, M.B. (2012). GIS-based modeling for location planning of jetties in coastal towns. Ocean & Coastal Management 56, 17-25. https://doi.org/10.1016/j.ocecoaman.2011.10.010.

IPCC (2007). Climate Change 2007: Impacts, adaptation, and vulnerability. contribution of Working Group II to the Forth Assessment Report of the Intergovernmental Panel on Climate Change. Cambridge, United Kingdom and New York, NY, USA: Cambridge University Press, https://doi.org/10.2134/jeq2008.0015br

Kermani S., Boutiba M., Guendouz M., Guettouche M.S. and Khelfani D. (2016). Detection and analysis of shoreline changes using geospatial tools and automatic computation: Case of jijelian sandy coast (East Algeria). Ocean & Coastal Management 132, 46-58. https://doi.org/10.1016/j.ocecoaman.2016.08.010.

Muthusankar G., Jonathan M.P., Lakshumanan C., Roy P.D. and Srinivasa-Raju K. (2016). Coastal erosion vs man-made protective structures: evaluating a two-decade history from southeastern India. Natural Hazards 85(1), 637-647. https://doi.org/10.1007/s11069-016-2583-7.

Natesan U., Parthasarathy A., Vishnunath R., Kumar G.E.J, and Ferrer V.A. (2015). Monitoring longterm shoreline changes along Tamil Nadu, India using geospatial techniques. Aquatic Procedia 4, 325-332. https://doi.org/10.1016/j.aqpro.2015.02.044.

Rahman A.F., Dragoni D., and El-Masri B. (2011). Response of the Sundarbans coastline to sea level rise and decreased sediment flow: A remote sensing assessment. Remote Sensing of Environment 115(12), 3121-3128. https://doi.org/10.1016/j.rse.2011.06.019.

Robinson E. (2004). Coastal changes along the coast of Vere, Jamaica over the past two hundred years: data from maps and air photographs. Quaternary International 120 (1), 153-161. https://doi.org/10.1016/j.quaint.2004.01.014.

Ryu J., Won J. and Min, K. (2002). Waterline extraction from Landsat TM data in a tidal flatA case study in Gomso Bay, Korea. Remote Sensing of Environment 83(3), 442-456. https://doi.org/10.1016/s0034-4257(02)00059-7.

Snoussi M., Ouchani T. and Niazi, S. (2008). Vulnerability assessment of the impact of sea-level rise and flooding on the Moroccan coast: The case of the Mediterranean eastern zone. Estuarine, Coastal and Shelf Science 77(2), 206-213. https://doi.org/10.1016/j.ecss.2007.09.024.

Tran Thi V., Tien Thi Xuan A., Phan Nguyen H., Dahdouh-Guebas F. and Koedam N. (2014). Application of remote sensing and GIS for detection of long-term mangrove shoreline changes in Mui Ca Mau, Vietnam. Biogeosciences 11(14), 3781-3795. https://doi.org/10.5194/bg-11-3781-2014.

Vinayaraj P., Johnson G., Udhaba Dora G., Sajiv Philip C., Sanil Kumar V. and Gowthaman R. (2011). Quantitative estimation of coastal changes along selected locations of Karnataka, India: A GIS and remote sensing approach. International Journal of Geosciences 02(04), 385-393. https://doi.org/10.4236/ijg.2011.24041.

Vongvisessomjai S., Polsi R., Manotham C., Srisaengthong D. and Charulukkana S. (1996). Coastal Erosion in the Gulf of Thailand. In: Sea-Level Rise and Coastal Subsidence. Coastal Systems and Continental Margins (J.D Milliman and B.U. Haq, Eds.) vol 2. Springer, Dordrecht. https://doi.org/10.1007/978-94-015-8719-8_.

White K. and El Asmar H.M. (1999). Monitoring changing position of coastlines using Thematic Mapper imagery, an example from the Nile Delta. Geomorphology 29(1-2), 93-105. https://doi.org/10.1016/s0169-555x(99)00008-2.

Yagoub M.M. and Kolan, G.R. (2006). Monitoring coastal zone land use and land cover changes of Abu Dhabi using remote sensing. Journal of the Indian Society of Remote Sensing 34 (1), 57-68. https://doi.org/10.1007/bf02990747.